

**Electronic Supplementary Information**

**Enhanced oxygen evolution activity of graphitic carbon shell embedded nickel/nickel  
oxide core-shell nanoparticles via surface dissolution**

*Chetna Madan<sup>1</sup> Dr. Chandra Sekhar Tiwary<sup>2</sup> and Aditi Halder<sup>1\*</sup>*

<sup>1</sup>School of Basic Sciences, Indian Institute of Technology Mandi, (H. P.), India-175005

<sup>2</sup>Department of Metallurgical and Materials Engineering, Indian Institute of Technology,  
Kharagpur, (W.B.), India-721302

Corresponding Author's Email: [aditi@iitmandi.ac.in](mailto:aditi@iitmandi.ac.in)

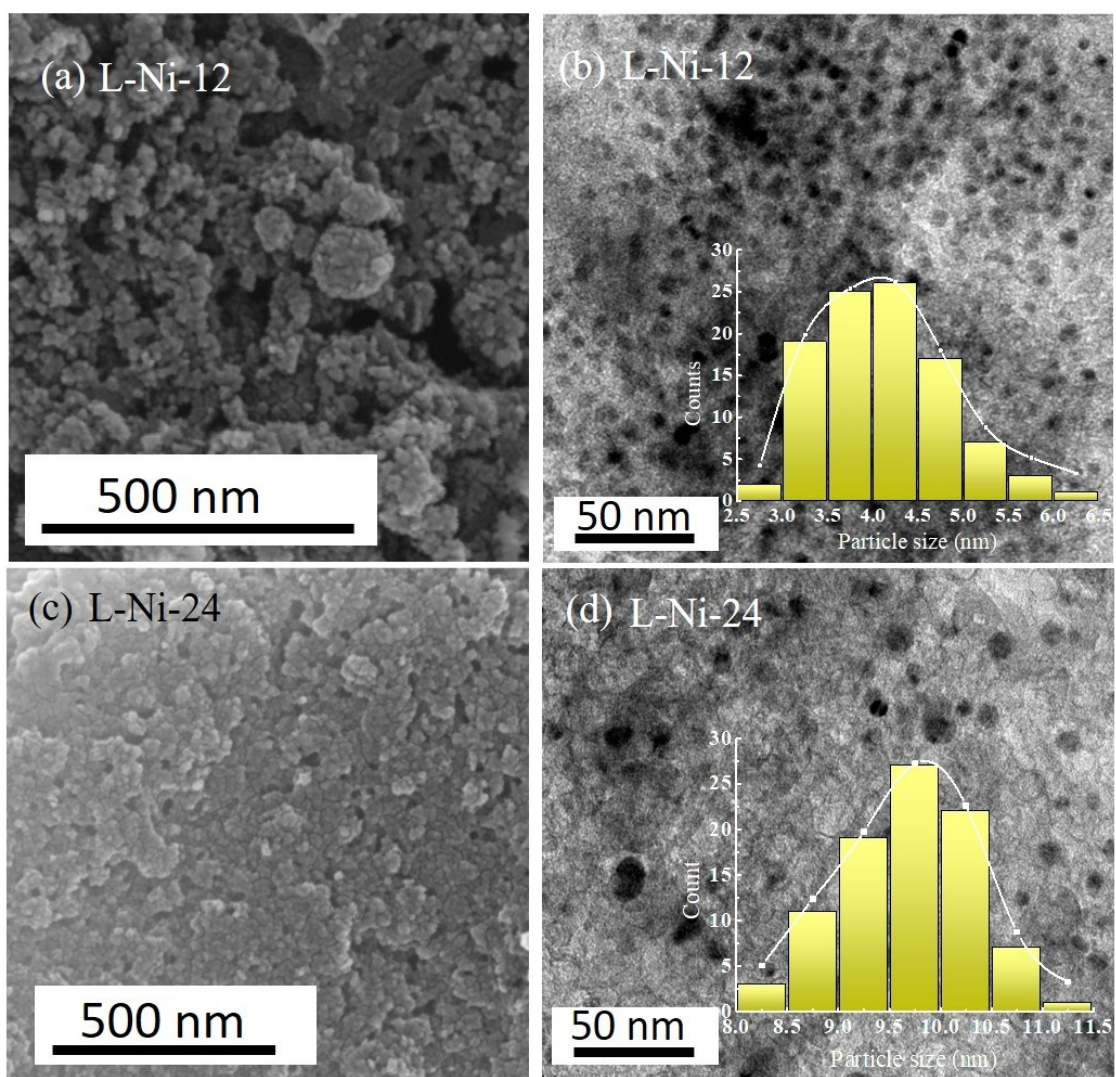


Figure S1: SEM images (a), (c) at low magnification showing the morphologies and particle size distribution plots from TEM images (b) and (d).

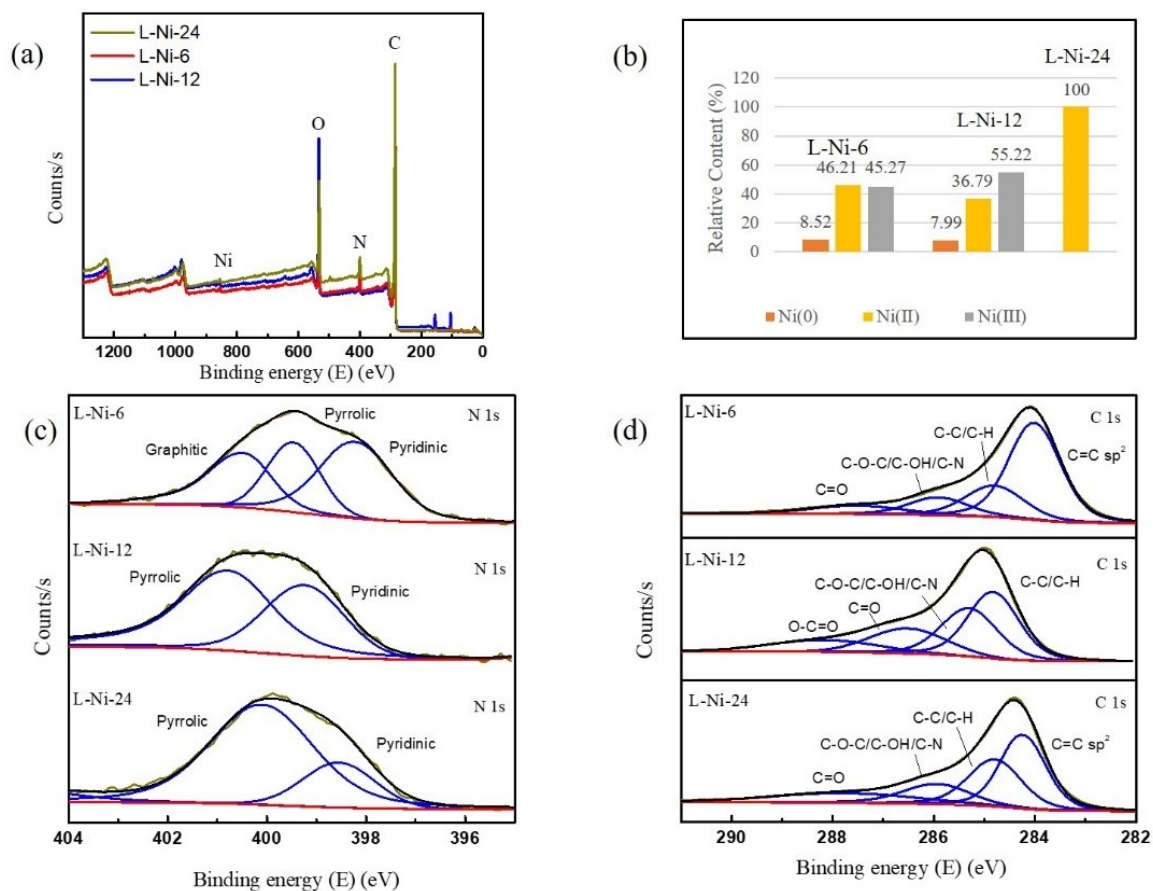


Figure S2: (a) XPS survey spectra of all the samples confirming the elements present. (b) Relative percentage of various oxidation states of nickel present in the samples (c) High-resolution N 1s spectra and (d) C 1s spectra.

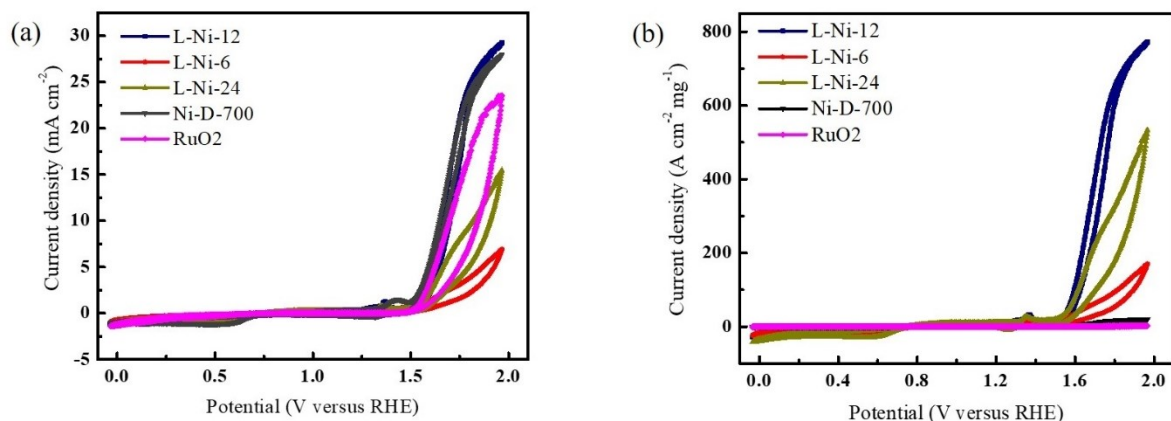


Figure S3: (a) Cyclic voltammograms swept at the scan rate of 20mV/s between 0 to 2V vs. RHE in  $N_2$  saturated 1 M KOH where current density is normalized against geometric surface area. (b) The same CV plots with current density normalized against the mass of the active metal present in each of the catalyst.

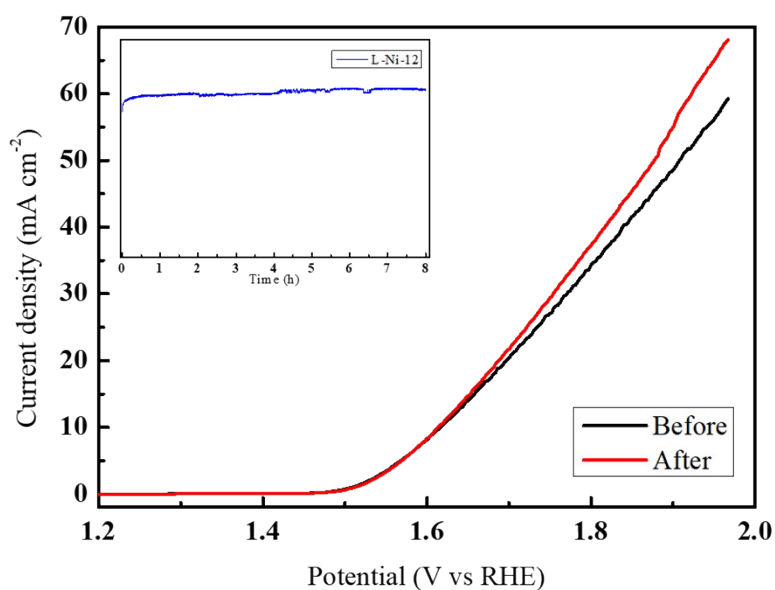


Figure S4: OER activity of the sample before and after 8 hours of Chronoamperometry test (inset) on L-Ni-12 at 1.55V vs. RHE in  $N_2$  saturated 1 M KOH.

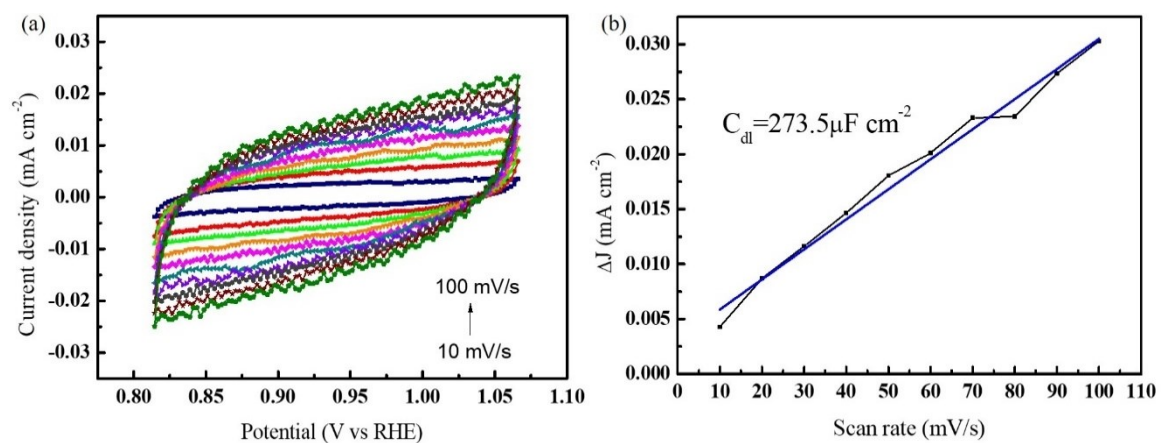


Figure S5: (a) Cyclic voltammograms were programmed at the scan rate of 10 to 100mV/s in the non-faradaic region for electrochemical double-layer measurements in N<sub>2</sub> saturated 1 M KOH. (b) Capacitive current density against scan rate where the slope gives C<sub>dl</sub> value for the catalyst L-Ni-12.

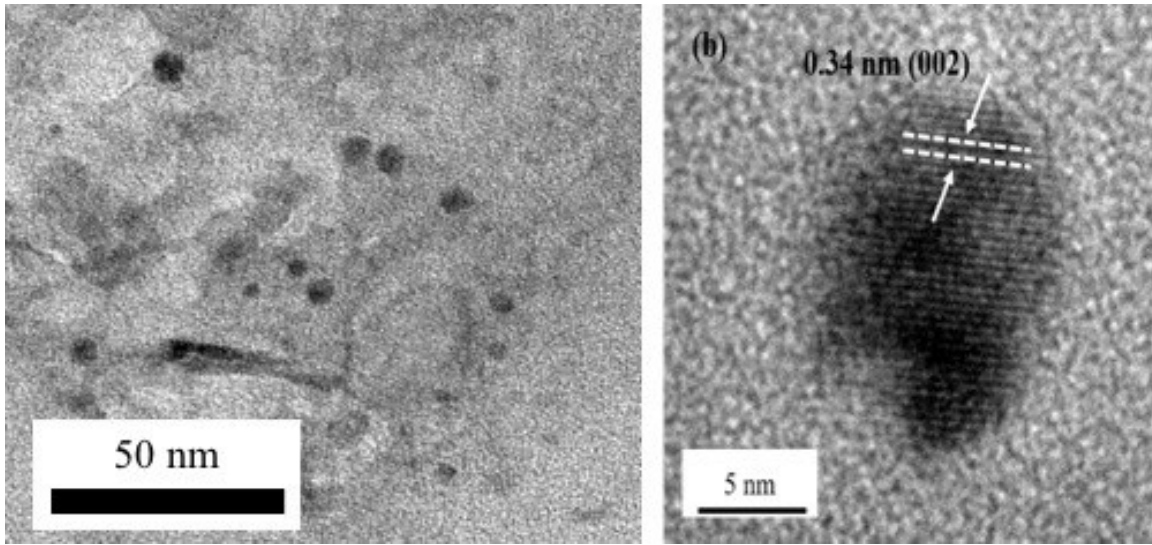


Figure S6: TEM image (a) and HR-TEM image (b) of L-Ni-12 after OER operation.

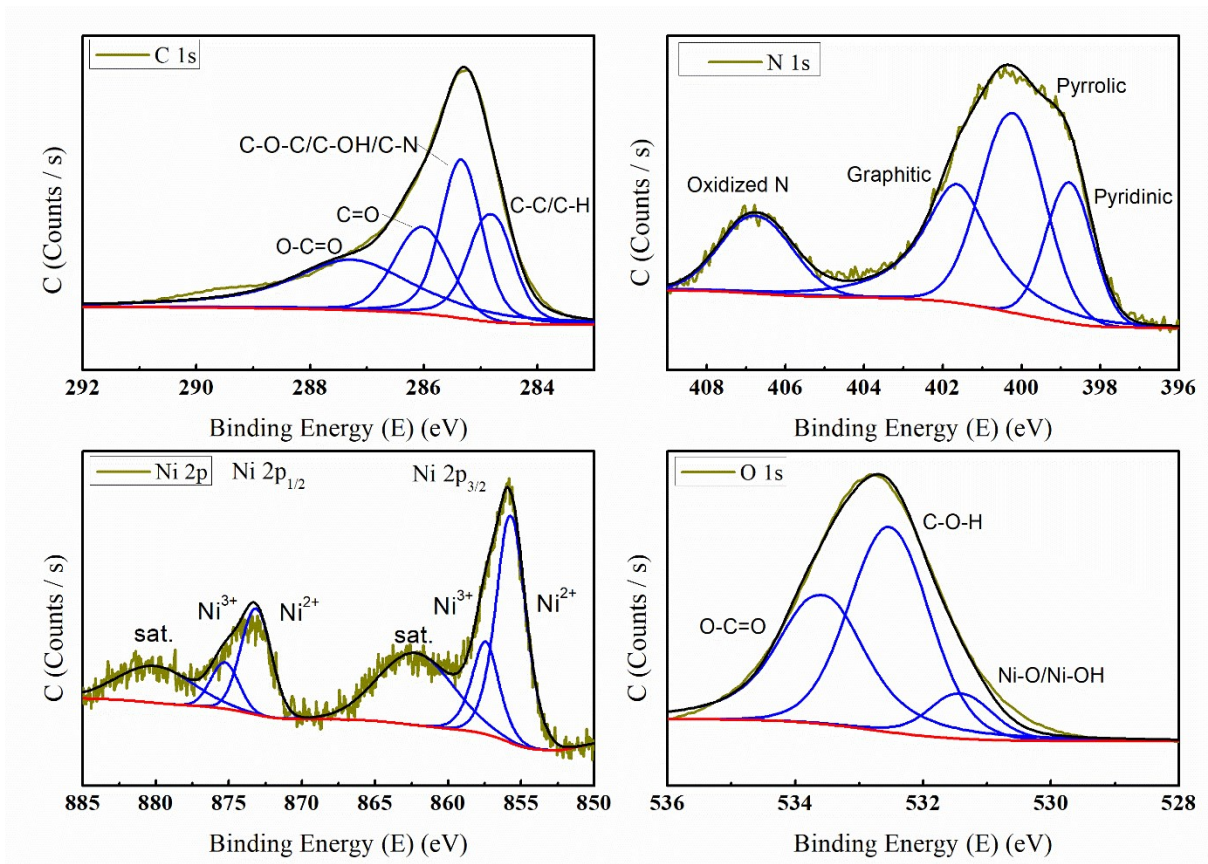


Figure S7: XPS results of L-Ni-12 post OER catalysis.

Sample	Onset potential (V vs. RHE)	Overpotential( $\eta$ ) at 10 mA cm <sup>-2</sup> (mV)	Tafel Slope (mV dec <sup>-1</sup> )	Charge transfer resistance ( $R_{ct}$ ) (ohms)
L-Ni-6	1.65	-	96.89	770
L-Ni-12	1.52	360	53.4	290
L-Ni-24	1.68	-	124.3	568
Ni-D-700	1.55	410	81.3	70
RuO <sub>2</sub>	1.51	390	-	-

Table S1: Summary of electrocatalytic performance of the samples.

Electrocatalyst	Mass Loading (mg cm <sup>-2</sup> )	Overpotential( $\eta$ ) at 10 mA cm <sup>-2</sup> (mV)	Tafel Slope (mV dec <sup>-1</sup> )	Electrolyte	Reference
Ni-NC700	0.31	430	66	0.1 MKOH	1
NiFeP@NPC	0.4	350	78	1 MKOH	2
NiFe <sub>2</sub> O <sub>4</sub>	2	381	46.5	1 MKOH	3
O-NiCoFe-LDH	0.12	430	60	0.1 MKOH	4
CoP@SNC	0.6	350	68	1 MKOH	5
CoP/Co-N-C/NPC	-	374	92	1 MKOH	6
Ni@NC-800	0.8	290	45	1 MKOH	7
NiCo <sub>2</sub> O <sub>4</sub>	-	440	164	0.1 MKOH	8
5%Ni-Co	0.4	381	72.5	0.1 MKOH	9
Ni <sub>3</sub> Fe/NC	0.13	370	77	0.1 MKOH	10
L-Ni-12	0.07	360	53.4	1 MKOH	This work

Table S2: Comparison of electrocatalytic performance of some of the related transition metal based electrocatalyst to our catalyst.

## **References:**

1. Devi, B., Koner, R. R. & Halder, A. Ni(II)-Dimeric Complex-Derived Nitrogen-Doped Graphitized Carbon-Encapsulated Nickel Nanoparticles: Efficient Trifunctional Electrocatalyst for Oxygen Reduction Reaction, Oxygen Evolution Reaction, and Hydrogen Evolution Reaction. *ACS Sustain. Chem. Eng.* **7**, 2187–2199 (2019).
2. Wang, J. & Ciucci, F. In-situ synthesis of bimetallic phosphide with carbon tubes as an active electrocatalyst for oxygen evolution reaction. *Appl. Catal. B Environ.* **254**, 292–299 (2019).
3. Maruthapandian, V., Mathankumar, M., Saraswathy, V., Subramanian, B. & Muralidharan, S. Study of the Oxygen Evolution Reaction Catalytic Behavior of  $\text{Co}_x\text{Ni}_{1-x}\text{Fe}_2\text{O}_4$  in Alkaline Medium. *ACS Appl. Mater. Interfaces* **9**, 13132–13141 (2017).
4. Qian, L. *et al.* Ternary Layered Double Hydroxides as High-Performance Bifunctional Materials for Oxygen Electrocatalysis. *Adv. Energy Mater.* **5**, 1–6 (2015).
5. Meng, T., Hao, Y. N., Zheng, L. & Cao, M. Organophosphoric acid-derived CoP quantum dots@S,N-codoped graphite carbon as a trifunctional electrocatalyst for overall water splitting and Zn-air batteries. *Nanoscale* **10**, 14613–14626 (2018).
6. Wang, S. *et al.* Cobalt–Tannin-Framework-Derived Amorphous Co–P/Co–N–C on N, P Co-Doped Porous Carbon with Abundant Active Moieties for Efficient Oxygen Reactions and Water Splitting. *ChemSusChem* **12**, 830–838 (2019).
7. Xu, Y. *et al.* Nickel Nanoparticles Encapsulated in Few-Layer Nitrogen-Doped Graphene Derived from Metal–Organic Frameworks as Efficient Bifunctional Electrocatalysts for Overall Water Splitting. *Adv. Mater.* **29**, 1–8 (2017).
8. Lee, D. U., Kim, B. J. & Chen, Z. One-pot synthesis of a mesoporous  $\text{NiCo}_2\text{O}_4$  nanoplatelet and graphene hybrid and its oxygen reduction and evolution activities as an efficient bi-functional electrocatalyst. *J. Mater. Chem. A* **1**, 4754–4762 (2013).
9. Song, W. *et al.* Ni- and Mn-Promoted Mesoporous  $\text{Co}_3\text{O}_4$ : A Stable Bifunctional Catalyst with Surface-Structure-Dependent Activity for Oxygen Reduction Reaction and Oxygen Evolution Reaction. *ACS Appl. Mater. Interfaces* **8**, 20802–20813 (2016).
10. Fu, G. *et al.*  $\text{Ni}_3\text{Fe-N}$  Doped Carbon Sheets as a Bifunctional Electrocatalyst for Air Cathodes. *Adv. Energy Mater.* **7**, 1–8 (2017).